

FULL PAPER

Influence of the C-terminal substituent on the crystal-state conformation of Adm peptides

Fatemeh M. Mir¹  | Marco Crisma²  | Claudio Toniolo^{2,3}  | William D. Lubell¹ 

¹Département de Chimie, Université de Montréal, Montréal, Québec, Canada

²Institute of Biomolecular Chemistry, Padova Unit, Padova, Italy

³Department of Chemistry, University of Padova, Padova, Italy

Correspondence

Claudio Toniolo, Department of Chemistry, University of Padova, via Marzolo 1, 35131 Padova, Italy.

Email: claudio.toniolo@unipd.it

William D. Lubell, Département de Chimie, Université de Montréal, C. P. 6128, Succursale Centre-Ville, Montréal, Québec, Canada H3C 3J7.

Email: william.lubell@umontreal.ca

Funding information

FRQNT Centre in Green Chemistry and Catalysis (CGCC), Grant/Award Number: Strategic Cluster RS-171310; Natural Sciences and Engineering Research Council of Canada (NSERC), Grant/Award Number: Discovery Grant RGPIN-06647; Université de Montréal

Abstract

The *bis*-functionalized diamondoid α -amino acid 2-aminoadamantane-2-carboxylic acid (Adm) has been used as the building block of four N^α -formyl homo-dipeptide alkylamide sequences *via* a solution-phase Ugi multicomponent reaction approach. The conformers of these peptides have been determined in the crystalline state by X-ray diffraction to distinguish the influences of the C-terminal substituent. One of the Adm peptides folds into an open and a hydrogen-bonded γ -turn geometry. Moreover, 3D-structures have been observed featuring two consecutive γ -turns in an incipient γ -helical structure, a significantly distorted nonhelical β -turn, as well as an S-shaped conformation with opposite helical screw senses. A significant topological variety is thus exhibited by the -Adm-Adm- sequences contingent on their C-terminal substituents, illustrating both the broad conformational potential and the need for further characterization of this sterically bulky residue in explorations of its ϕ , ψ space.

KEYWORDS

2-aminoadamantane-2-carboxylic acid peptides, crystal-state conformation, β -turn, γ -helix, γ -turn

1 | INTRODUCTION

$C^{\alpha\alpha}$ -Dialkylglycines have the potential for restricting backbone conformation within peptide chains. For example, numerous 3D-structural analyses of α -aminoisobutyric acid (Aib) residues^[1–6] in different peptides in solution and in the crystal state have demonstrated the strong tendency for this achiral amino acid to induce type-III (III') β -turn^[7–12] and 3_{10} -/ α -helical conformations.^[1–4,13,14] Although $C^{\alpha\alpha}$ -cycloalkyl α -amino acid residues (e.g., 1-aminocyclopentane-1-carboxylic acid, Ac₅C, and 1-aminocyclohexane-1-carboxylic acid, Ac₆C)^[15] exhibit similar propensity, as the bulkiness of both $C^{\alpha\alpha}$ -substituents increases in acyclic α -amino acids of this class (e.g., $C^{\alpha\alpha}$ -diethylglycine, Deg), the fully extended conformation becomes more stable.^[16–18]

The diamondoid^[19–22] 2-aminoadamantane-2-carboxylic acid (Adm) residue has shown intriguing potential for adopting the relatively uncommon γ -turn conformation^[23–29] in X-ray diffraction studies of short Adm-rich peptides and homo-peptides.^[30,31] In

solution,^[32] Adm derivatives and dipeptides, such as Ac-Adm-NHMe (Ac, acetyl; NHMe, methylamino) and Ac-Adm-Gly-NHMe, have been suggested to fold in γ -turn conformations based on NMR and IR absorption spectroscopic studies. Moreover, certain Adm homo-peptides^[30,31] have been observed by X-ray diffraction to exhibit two consecutive, regular γ -turns, indicating the possibility to form the still uncharacterized γ -helix.^[33]

The influences of the C-terminal substituent on the tendency of the -Adm-Adm- dipeptide sequence to adopt the γ -turn conformation have now been investigated by the synthesis and X-ray diffraction analysis of a series of di- and tripeptides N-terminating in a common formyl group. The sequences listed below feature different C-terminal substituents to specifically examine the role of size and hydrogen-bond donor and acceptor units: HCO-(Adm)₂-Gly-OEt (**4a**), HCO-(Adm)₂-NHtPr (**4b**), HCO-(Adm)₂-NHtBu (**4c**), and HCO-(Adm)₂-Aib-OMe (**4d**). In addition, the X-ray diffraction structure of a strictly related dipeptide, HCO-Adm-Aib-OMe (**2d**), has been also solved and studied.

2 | EXPERIMENTAL

2.1 | Synthesis and characterization

Dichloromethane (DCM) and methanol (MeOH) were used after drying by passage through solvent filtration systems (GlassContour, Irvine, CA). Reagents from commercial sources were used as received. Purification by silica gel chromatography was performed on 230-400 mesh silica gel. Analytical thin-layer chromatography was carried out on silica gel 60 F254 (Aluminum Sheet) and visualized by UV absorbance or by staining with iodine. Melting points were obtained on sample in capillary tubes using a Mel-Temp melting point apparatus and reported in degree Celsius (°C). Infrared absorption spectra were recorded on a Bruker Alpha P FT-IR spectrophotometer equipped with a single reflection ATR sampling module that allows spectral acquisition from neat solid and liquid samples. The frequency of absorption is reported in reciprocal centimeters (cm⁻¹). ¹H and ¹³C NMR spectra were recorded at room temperature (rt) in CDCl₃ (7.26 ppm/77.16 ppm) or in deuterated dimethylsulfoxide (DMSO, *d*₆) (2.50 ppm/39.52 ppm) on Bruker AV (300/75 and 500/125 MHz) instruments and referenced to internal solvent. Chemical shifts are reported in parts per million (ppm); coupling constants (*J* values) in Hertz; abbreviations for peak multiplicities are s (singlet), d (doublet), t (triplet), q (quadruplet), m (multiplet) and br (broad). High-resolution mass spectrometry (HRMS) was performed by the Centre Régional de Spectroscopie de Masse de l'Université de Montréal, using protonated molecular ions [M + H]⁺, [M + 2H]²⁺ or sodium adducts [M + Na]⁺ for empirical formula confirmation.

HCO-Gly-OEt. A mixture of HCl · H-Gly-OEt (10.0 g, 70 mmol) and ammonium formate (9.20 g, 146 mmol, 2.1 eq) in CH₃CN (75 mL) was heated at reflux and stirred for 16 hours. The volatiles were removed under reduced pressure. The residue was partitioned between water (30 mL) and DCM (30 mL). The layers were separated. The aqueous phase was extracted with DCM (2 × 30 mL). The combined organic layer was dried over Na₂SO₄ and filtered. The filtrate was concentrated to provide HCO-Gly-OEt as a pale-yellow liquid (6.98 g, 53.2 mmol, 76%) that was used without further purification. *R*_f 0.33 (1:4 hexane: ethyl acetate, EtOAc). ¹H NMR (500 MHz, CDCl₃): δ 1.21 (t, *J* = 7.0 Hz, 3H); 3.98 (d, *J* = 6.0 Hz, 2H), 4.14 (q, *J* = 7.2 Hz, 2H), 6.85 (br, 1H), 8.17 (s, 1H) ppm. ¹³C NMR (125 MHz, CDCl₃): δ 14.0, 39.9, 61.6, 161.6, 169.6 ppm. HRMS (ESI): *m/z* calcd for C₅H₁₀NO₃ 132.0655; found [M + H]⁺ 132.0657.

HCO-Aib-OMe.^[34–36] A solution of H-Aib-OH (5.0 g, 48.5 mmol) in MeOH (25 mL) was cooled to 0 °C, treated with SOCl₂ (7.0 mL, 97 mmol, 2 eq) and left to stir for 16 hours with warming to rt. The volatiles were removed under reduced pressure to give HCl·H-Aib-OMe as a white solid in quantitative yield. The salt was dissolved in formic acid (15 mL), treated with a solution of sodium formate (3.21 g, 50.9 mmol, 1.05 eq) in a minimum amount of formic acid, and left to stir at 40 °C. After 2 hours, the mixture was filtered, and the filtrate was treated with 1:1 formic acid: acetic anhydride (4 mL/15 mL), heated to 80 °C and stirred for 20 hours. The mixture was filtered and the filtrate was concentrated under vacuum to give HCO-Aib-OMe as a pale-yellow oil, which exhibited the same characteristics as

previously reported. ¹H NMR (300 MHz, CDCl₃): δ 1.58 (s, 6H), 3.74 (s, 3H), 6.68 (s, 1H), 8.10 (s, 1H) ppm.

Ethyl isocyanoacetate (1a). HCO-Gly-OEt (5.7 g, 43.5 mmol) in DCM (43 mL) was treated with triethylamine (TEA) (13.2 g, 130.5 mmol, 3 eq), cooled to –5 °C and treated dropwise with POCl₃ (8 g, 52.2 mmol, 1.2 eq). After stirring at –5 °C for 1 hour, the resulting reddish mixture was treated with a solution of sat. NaHCO₃ (30 mL) and agitated thoroughly. The organic phase was separated, washed with brine, dried over Na₂SO₄, filtered, and evaporated under reduced pressure to afford a reddish liquid, which was purified by column chromatography using an eluent of hexane:EtOAc (7:3). Evaporation of the collected fractions gave isocyanide **1a** as pale-yellow oil (3.6 g, 31.8 mmol, 73%). *R*_f 0.48 (7:3 hexane:EtOAc). ¹H NMR (500 MHz, CDCl₃): δ 1.28 (t, *J* = 7.0 Hz, 3H), 4.20 (s, 2H), 4.24 (q, *J* = 7.0 Hz, 2H) ppm. ¹³C NMR (125 MHz, CDCl₃): δ 14.0, 43.5, 62.7, 161.0, 164.0 ppm. IR absorption (ATR): ν 2162, 1750; HRMS (ESI): *m/z* calcd for C₅H₈NO₂ 114.0555; found [M + H]⁺ 114.0551.

Methyl 2,2-dimethyl-isocyanoacetate (1d).^[35] This compound was synthesized according to the procedure described above for **1a** using HCO-Aib-OMe (7.5 g, 49.2 mmol), TEA (24.3 mL, 246 mmol, 5 eq), and POCl₃ (6.9 mL, 73.8 mmol, 1.5 eq) at –20 °C. Evaporation of the volatiles gave an orange liquid that was purified by column chromatography using hexane:EtOAc (7:3) as eluent to furnish isocyanide **1d** (3.75 g, 29.5 mmol, 60%) as a pale-yellow liquid that exhibited the same characteristics as previously reported. *R*_f 0.72 (3:7 hexane:EtOAc); ¹H NMR (300 MHz, CDCl₃): δ 1.64 (s, 6H), 3.80 (s, 3H) ppm. ¹³C NMR (75 MHz, CDCl₃): δ 27.5, 53.6, 59.5, 157.9, 170.1 ppm.

HCO-Adm-Gly-OEt (2a). A solution of isocyanoacetate **1a** (3 g, 26.5 mmol) in MeOH (2 M) was treated with adamantan-2-one (3.98 g, 26.5 mmol, 1 eq) followed by a solution of ammonium formate (2.0 g, 31.8 mmol, 1.2 eq) in the minimum amount of water, and stirred for 24 hours. The volatiles were evaporated. The residue was dissolved in CHCl₃, washed with water and brine, dried over Na₂SO₄, and evaporated to a residue that was purified on column chromatography using hexane:EtOAc (1:1) as eluent to provide dipeptide **2a** (1.52 g, 4.92 mmol, 56%) as a powder: *R*_f 0.34 (1:1 hexane:EtOAc); m. p. 165.2–167.2 °C; ¹H NMR (300 MHz, CDCl₃): δ 1.26 (t, *J* = 7.2 Hz, 3H); 1.67 (m, 1H), 1.71 (m, 3H), 1.76 (m, 2H), 1.83–1.84 (m, 2H), 1.94–2.04 (m, 4H), 2.68 (m, 2H), 3.99 (d, *J* = 5.8 Hz, 2H), 4.17 (q, *J* = 7.1 Hz, 2H), 5.82 (s, 1H), 7.59 (t, *J* = 5.7 Hz, 1H), 8.13 (d, *J* = 2.0 Hz, 1H) ppm. ¹³C NMR (75 MHz, CDCl₃): δ 14.3, 26.5, 26.6, 32.2, 32.5, 33.9, 37.4, 41.5, 61.4, 64.9, 161.9, 169.9, 172.8 ppm. IR absorption (ATR): ν 3254, 1746, 1682, 1641, 1531; HRMS (ESI): *m/z* calcd for C₁₆H₂₅N₂O₄ 309.1809; found [M + H]⁺ 309.1818.

HCO-Adm-NHiPr (2b). This compound was synthesized from isopropyl isocyanide (**1b**, 1.0 g, 14.5 mmol) according to the procedure described above for the synthesis of dipeptide **2a** and purified by column chromatography using hexanes:EtOAc (3:2) as eluent. The collected fractions were evaporated to give **2b** as a powder (2.4 g, 9.1 mmol, 63%); *R*_f 0.33 (3:97 MeOH:DCM); m.p. 181–185 °C; ¹H NMR (500 MHz, CDCl₃): δ 1.13 (d, *J* = 6.5 Hz, 6H), 1.65–1.74 (m, 6H), 1.80–1.82 (m, 2H), 1.92–1.96 (m, 4H), 2.64 (br, 2H), 4.01–4.07 (m, 1H),

6.07 (s, 1H), 6.96 (d, $J = 7.5$ Hz, 1H), 8.12 (d, $J = 2.5$ Hz, 1H) ppm. ^{13}C NMR (125 MHz, CDCl_3): δ 22.6, 26.5, 26.6, 32.1, 32.6, 34.0, 37.4, 41.4, 64.9, 161.7, 171.2 ppm. IR absorption (ATR): ν 3320, 3286, 1652, 1518; HRMS (ESI): m/z calcd for $\text{C}_{15}\text{H}_{25}\text{N}_2\text{O}_2$ 265.1911; found $[\text{M} + \text{H}]^+$ 265.1916.

HCO-Adm-NHtBu (2c). This compound was synthesized from *tert*-butyl isocyanide (**1c**, 3.0 g, 41.6 mmol) according to the procedure described above for the synthesis of dipeptide **2a** and purified by column chromatography using hexane:EtOAc (7:3) as eluent. The collected fractions were evaporated to give **2c** as a powder (8.3 g, 29.8 mmol, 72%); R_f 0.2 (7:3 hexane:EtOAc); m.p. 197–200 °C; ^1H NMR (500 MHz, CDCl_3): δ 1.32 (s, 9H), 1.63–1.72 (m, 6H), 1.79–1.84 (m, 2H), 1.92–2.00 (m, 4H), 2.60 (br, 2H), 6.16 (s, 1H), 6.95 (s, 1H), 8.11 (d, $J = 2.0$ Hz, 1H) ppm. ^{13}C NMR (125 MHz, CDCl_3): δ 26.4, 26.6, 28.6, 32.1, 32.6, 34.1, 37.3, 51.0, 65.4, 161.7, 171.0 ppm. IR absorption (ATR): ν 3264, 1674, 1649, 1540; HRMS (ESI): m/z calcd for $\text{C}_{16}\text{H}_{27}\text{N}_2\text{O}_2$ 279.2067; found $[\text{M} + \text{H}]^+$ 279.2066.

HCO-Adm-Aib-OMe (2d). This compound was synthesized according to the procedure described above for the synthesis of dipeptide **2a** using methyl 2,2-dimethyl-isocyanoacetate **1d** (1.27 g, 10.0 mmol), adamantan-2-one (1.5 g, 10.0 mmol, 1 eq), and ammonium formate (0.95 g, 15.0 mmol, 1.5 eq). The residue was purified on column chromatography using hexanes:EtOAc (7:3) as eluent to give dipeptide **2d** as a powder (1.98 g, 6.1 mmol, 62%); R_f 0.50 (1:9 MeOH:EtOAc); m.p. 185.8–189.5 °C; ^1H NMR (300 MHz, CDCl_3): δ 1.48 (s, 6H), 1.66 (m, 1H), 1.70 (m, 4H), 1.75 (m, 1H), 1.82 (m, 2H), 1.92–2.01 (m, 4H), 2.65 (m, 2H), 3.68 (s, 3H), 5.70 (s, 1H), 7.57 (s, 1H), 8.15 (d, $J = 2.0$ Hz, 1H) ppm. ^{13}C NMR (75 MHz, CDCl_3): δ 25.0, 26.5, 26.7, 32.1, 32.5, 33.9, 37.3, 52.4, 56.0, 64.9, 161.9, 171.2, 174.9 ppm. HRMS (ESI): m/z calcd for $\text{C}_{17}\text{H}_{27}\text{N}_2\text{O}_4$ 323.1965, found $[\text{M} + \text{H}]^+$ 323.1976.

"CN-Adm"-Gly-OEt (3a) was synthesized from dipeptide **2a** (1.51 g, 4.68 mmol) according to procedure described above for the synthesis of isocyanoacetate **1a**. The volatiles were removed and the orange residue was purified by column chromatography using hexane:EtOAc (7:3) as eluent to afford isocyanide **3a** as a white powder (1.03 g, 3.5 mmol, 72%). R_f 0.35 (7:3 hexane:EtOAc); m.p. 87.6–90.8 °C; ^1H NMR (500 MHz, CDCl_3): δ 1.28 (t, $J = 7.2$ Hz, 3H), 1.72 (m, 2H), 1.77–1.82 (m, 5H), 1.90–1.91 (m, 1H), 1.98–2.01 (m, 2H), 2.23–2.26 (m, 2H), 2.38 (m, 2H), 4.06 (d, $J = 5.3$ Hz, 2H), 4.22 (q, $J = 7.2$ Hz, 2H), 6.56 (br, 1H) ppm. ^{13}C NMR (125 MHz, CDCl_3): δ 14.2, 26.1, 26.3, 33.2 (2C), 34.9, 37.2, 41.7, 61.8, 68.5, 158.7, 167.8, 169.5 ppm. IR absorption (ATR): ν 3377, 2120, 1744, 1659, 1525; HRMS (ESI): m/z calcd for $\text{C}_{16}\text{H}_{23}\text{N}_2\text{O}_3$ 291.1703; found $[\text{M} + \text{H}]^+$ 291.1709.

"CN-Adm"-NHtPr (3b) was synthesized from HCO-Adm-NHiPr **2b** (2 g, 7.6 mmol) according to the procedure described above for the synthesis of isocyanoacetate **1a** at -5 °C. The resulting orange solid was purified by column chromatography using hexane:EtOAc (7:3) as eluent. The collected fractions were evaporated to give isocyanide **3b** as a white powder (1.70 g, 6.9 mmol, 90%); R_f 0.53 (7:3 hexane:EtOAc); m.p. 130–133 °C; ^1H NMR (500 MHz, CHCl_3): δ 1.18 (d, $J = 7.0$ Hz, 6H), 1.72 (m, 2H), 1.76–1.78 (m, 4H), 1.81 (m, 1H), 1.89–1.91 (m, 1H), 1.96–1.99 (m, 2H), 2.23–2.26 (m, 2H), 2.31 (m, 2H), 4.07–4.14 (m, 1H),

5.74 (br, 1H) ppm. ^{13}C NMR (125 MHz, CDCl_3): δ 22.4, 26.2, 26.4, 33.3 (2C), 35.0, 37.3, 42.1, 68.6, 158.2, 166.7 ppm. IR absorption (ATR): $\nu = 3315, 2122, 1647, 1533$; HRMS (ESI): m/z calcd for $\text{C}_{15}\text{H}_{23}\text{N}_2\text{O}$ 247.1805; found $[\text{M} + \text{H}]^+$ 247.1810.

"CN-Adm"-NHtBu (3c) was synthesized from HCO-Adm-NHtBu **2c** (6.75 g, 24.24 mmol) according to the procedure described above for the preparation of isocyanoacetate **1a** at -5 °C. The resulting yellow powder was purified by column chromatography using hexane:EtOAc (9:1) as eluent to afford isocyanide **3c** as a white powder (6.0 g, 23.0 mmol, 94%); R_f 0.36 (9:1 hexane:EtOAc); m.p. 116–120 °C; ^1H NMR (500 MHz, CHCl_3): δ 1.37 (s, 9H), 1.71 (m, 2H), 1.75–1.77 (m, 4H), 1.81 (m, 1H), 1.89 (m, 1H), 1.94–1.97 (m, 2H), 2.22–2.24 (m, 2H), 2.28 (m, 2H), 5.69 (s, 1H) ppm. ^{13}C NMR (125 MHz, CDCl_3): δ 26.2, 26.3, 28.5, 33.3, 35.1, 37.2, 39.4, 51.8, 68.9, 158.0, 166.6 ppm. IR absorption (ATR): ν 3363, 2120, 1660, 1527; HRMS (ESI): m/z calcd for $\text{C}_{16}\text{H}_{25}\text{N}_2\text{O}$ 261.19614; found $[\text{M} + \text{H}]^+$ 261.19712.

"CN-Adm"-Aib-OMe (3d) was synthesized from dipeptide **2d** (1.51 g, 4.68 mmol) according to the procedure described above for the synthesis of isocyanoacetate **1a** and purified by column chromatography using hexane:EtOAc (7:3) as eluent to afford isocyanide **3d** as a powder (1.31 g, 4.3 mmol, 92%); R_f 0.56 (7:3 hexane:EtOAc); m.p. 115.9–117.4 °C; ^1H NMR (300 MHz, CDCl_3): δ 1.58 (s, 6H), 1.72 (m, 2H), 1.75–1.81 (m, 5H), 1.89–1.90 (m, 1H), 1.94–1.97 (m, 2H), 2.22–2.25 (m, 2H), 2.33 (m, 2H), 3.74 (s, 3H), 6.55 (s, 1H) ppm. ^{13}C NMR (75 MHz, CDCl_3): δ 24.4, 26.2, 26.3, 33.1, 33.2, 34.9, 37.2, 52.9, 56.9, 68.6, 158.4, 166.6, 174.8 ppm. IR absorption (ATR): ν 3372, 2126, 1726, 1675, 1529; HRMS (ESI): m/z calcd for $\text{C}_{17}\text{H}_{25}\text{N}_2\text{O}_3$ 305.1860; found $[\text{M} + \text{H}]^+$ 305.1869.

HCO-(Adm)₂-Gly-OEt (4a) was synthesized from isocyanide **3a** (1.0 g, 3.43 mmol) according to the procedure described above for the synthesis of dipeptide **2a** and purified by column chromatography using hexane:EtOAc (3:7) as eluent to give tripeptide **4a** as a powder (1.1 g, 2.3 mmol, 67%); R_f 0.35 (3:7 hexane:EtOAc); m.p. 197–200 °C; ^1H NMR (500 MHz, DMSO): δ 1.17 (t, $J = 7.1$ Hz, 3H), 1.52–1.54 (m, 4H), 1.57–1.64 (m, 8H), 1.72–1.83 (m, 5H), 1.88–1.95 (m, 6H), 2.01–2.08 (m, 2H), 2.56–2.58 (m, 3H), 3.75 (d, $J = 2.5$ Hz, 2H), 4.06 (q, $J = 7.1$ Hz, 2H), 7.25 (s, 1H), 7.77 (t, $J = 5.7$ Hz, 1H), 7.97 (d, $J = 2.1$ Hz, 1H), 8.08 (d, $J = 1.8$ Hz, 1H) ppm. ^{13}C NMR (125 MHz, DMSO): δ 14.0, 25.9, 26.0, 26.2, 26.4, 31.3, 31.7, 32.2, 32.3, 33.3 (2C), 37.1, 37.3, 41.0, 60.2, 62.8, 64.1, 161.5, 170.0, 171.4, 172.1 ppm. IR absorption (ATR): ν 3275, 1761, 1650, 1513; HRMS (ESI): m/z calcd for $\text{C}_{27}\text{H}_{39}\text{N}_3\text{O}_5\text{Na}$ 508.2782; found $[\text{M} + \text{Na}]^+$ 508.2774.

HCO-(Adm)₂-NHtPr (4b) was synthesized from isocyanide **3b** (1.6 g, 6.47 mmol) according to the procedure described above for the synthesis of dipeptide **2a** and purified by column chromatography using hexane:EtOAc (2:3) as eluent to afford dipeptide **4b** as a powder (2.5 g, 5.7 mmol, 87%); R_f 0.25 (2:3 hexane:EtOAc); m.p. 192–198 °C; ^1H NMR (500 MHz, CHCl_3): δ 1.10 (d, $J = 6.6$ Hz, 6H), 1.62 (m, 1H), 1.65 (m, 1H), 1.69–1.70 (m, 9H), 1.76 (m, 1H), 1.79–1.83 (m, 4H), 1.93–1.95 (m, 6H), 2.00 (m, 1H), 2.03 (m, 1H), 2.64–2.66 (m, 4H), 3.99–4.07 (m, 1H), 5.74 (s, 1H), 6.81 (d, $J = 7.9$ Hz, 1H), 6.92 (s, 1H), 8.13 (d, $J = 1.9$ Hz, 1H) ppm. ^{13}C NMR (125 MHz, CDCl_3): δ 22.8, 26.4, 26.6

(2C), 26.9, 32.2, 32.6, 32.7, 32.8, 34.0, 34.2, 37.3, 37.7, 41.1, 64.7, 65.3, 161.3, 171.2, 172.1 ppm. IR absorption (ATR): ν 3360, 1677, 1511; HRMS (ESI): m/z calcd for $C_{26}H_{40}N_3O_3$ 442.3060; found $[M + H]^+$ 442.3073.

HCO-(Adm)₂-NHtBu (4c) was synthesized from isocyanide **3c** (2.0 g, 7.65 mmol) according to the procedure described above for the synthesis of dipeptide **2a** and purified by column chromatography using hexane:EtOAc (7:3) as eluent to give dipeptide **4c** as a powder (2.96 g, 6.5 mmol, 85%): R_f 0.21 (7:3 hexane:EtOAc); m.p. 228–230 °C; 1H NMR (500 MHz, $CDCl_3$): δ 1.30 (s, 9H), 1.62 (m, 1H), 1.64 (m, 1H), 1.68–1.72 (m, 8H), 1.75 (m, 1H), 1.78–1.82 (m, 5H), 1.94–1.96 (m, 6H), 2.00 (m, 1H), 2.03 (m, 1H), 2.63 (m, 2H), 2.68 (m, 2H), 5.55 (s, 1H), 6.83 (s, 1H), 6.93 (s, 1H), 8.13 (d, $J = 1.9$ Hz, 1H) ppm. ^{13}C NMR (125 MHz, $CDCl_3$): δ 26.3, 26.5, 26.6, 26.9, 28.8, 32.3, 32.6, 32.7, 32.8, 34.1, 34.2, 37.3, 37.6, 50.7, 65.3, 65.4, 161.0, 170.9, 171.9 ppm. IR absorption (ATR): ν 3256, 1684, 1655, 1538; HRMS (ESI): m/z calcd for $C_{27}H_{42}N_3O_3$ 456.3221; found $[M + H]^+$ 456.3242.

HCO-(Adm)₂-Aib-OMe (4d) was synthesized from isocyanide **3d** (1.0 g, 3.3 mmol) according to the procedure described above for the synthesis of dipeptide **2a** and purified by column chromatography using hexane:EtOAc (7:3) as eluent to give tripeptide **4d** as a powder (1.03 g, 2.1 mmol, 62%): R_f 0.34 (1:9 MeOH:EtOAc); m.p. 198–203 °C; 1H NMR (500 MHz, $CDCl_3$): δ 1.44 (s, 6H), 1.61–1.64 (m, 2H), 1.68–1.70 (m, 8H), 1.74–1.83 (m, 6H), 1.93–1.98 (m, 6H), 2.02–2.05 (m, 2H), 2.64 (m, 2H), 2.68 (m, 2H), 3.66 (s, 3H), 5.66 (s, 1H), 6.94 (s, 1H), 7.55 (s, 1H), 8.12 (d, $J = 1.9$ Hz, 1H) ppm. ^{13}C NMR (125 MHz, $CDCl_3$): δ 25.1, 26.3, 26.5, 26.6, 26.9, 32.3, 32.5, 32.6, 32.7, 34.0 (2C), 37.3, 37.6, 52.3, 55.7, 64.6, 65.5, 161.6, 171.2, 172.4, 175.0 ppm. IR absorption (ATR): ν 3285, 1739, 1677, 1650, 1524; HRMS (ESI): m/z calcd for $C_{28}H_{42}N_3O_5$ 500.3119; found $[M + H]^+$ 500.3133.

2.2 | X-Ray diffraction

Single crystals, suitable for X-ray diffraction analysis, of di- and tripeptides **2d** and **4a-d** were obtained from ethyl acetate (**2d**), acetone (**4a** and **4c**), DCM (**4b**), and DCM/hexane (**4d**).

X-Ray diffraction data for peptide **2d** were collected with a Gemini E four-circle kappa diffractometer (Agilent Technologies) equipped with a 92-mm EOS CCD detector, using graphite monochromated $Cu K\alpha$ radiation ($\lambda = 1.54178$ Å). Data collection and reduction were performed with the CrysAlisPro software (Agilent Technologies). A semi-empirical absorption correction based on the multi-scan technique using spherical harmonics was implemented in the SCALE3 ABSPACK scaling algorithm.

X-Ray diffraction data collection for the remaining four structures (**4a-d**) was performed at the Laboratoire de Diffraction des Rayons X de l'Université de Montréal with a Bruker Venture Metaljet diffractometer, equipped with a Gallium Liquid Metal Jet Source (Ga $K\alpha$ radiation, $\lambda = 1.34139$ Å), Helios MX Mirror Optics, a kappa goniometer, and a Photon 100 CMOS detector. Data collection, data reduction, and absorption correction were achieved by use of the APEX 2, SAINT,

and SADABS (or TWINABS where appropriate) software packages (Bruker AXS).

The structures were solved by ab initio procedures of the SIR 2014^[37] or SHELXT^[38] programs, and refined by full-matrix least-squares procedures on F^2 , using all data, by application of the SHELXL-2014^[39] or OLEX2^[40] programs, with anisotropic displacement parameters for all of the nonhydrogen atoms. Hydrogen atoms were calculated at idealized positions and refined using a riding model.

Relevant crystal data and structure refinement parameters are reported in Tables S1–S5. CCDC 1880257–1880261 contain the supplementary crystallographic data for this article. The data can be obtained free of charge from The Cambridge Crystallographic Data Centre via www.ccdc.cam.ac.uk/structures.

3 | RESULTS

3.1 | Peptide synthesis

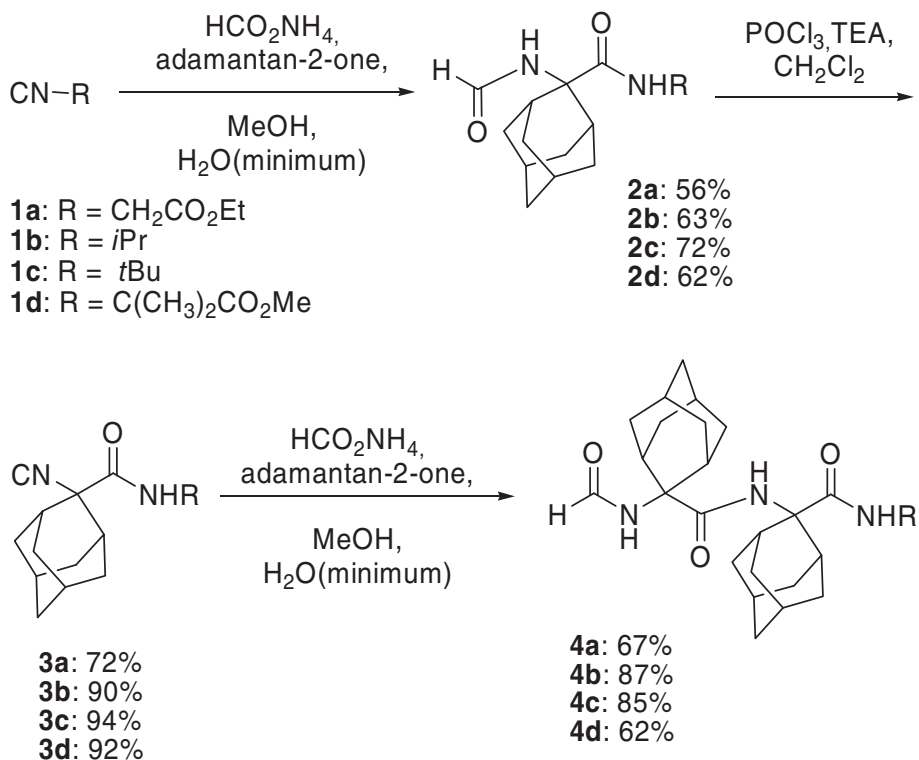
$C^{\alpha,\alpha}$ -Disubstituted glycines are generally recalcitrant to peptide bond formation because of their remarkable steric hindrance. This phenomenon becomes particularly significant in coupling reactions to their α -amino functionality.^[41,42] These unfavorable properties are magnified in couplings to Adm residues due to the increased bulkiness of this diamondoid residue.^[19–22]

Among the different methods examined for coupling $C^{\alpha,\alpha}$ -disubstituted glycines, the Ugi multicomponent reaction^[35,43] employing the commercially available 2-adamantanone, ammonium formate, and different isonitriles (CN-R) was found to furnish Adm derivatives and peptides in relatively high yields (Scheme 1). Four isonitriles **1a-d** were investigated to begin the synthesis of a series of Adm dipeptides possessing various C-terminal residues: *iso*-propyl and *tert*-butyl isonitriles **1b** and **1c** were obtained from commercial sources; α -amino ester-derived isonitriles **1a** and **1d** were respectively synthesized by formylation using ammonium formate and acetic anhydride, followed by isonitrile formation using $POCl_3$ and TEA. Adamantan-2-one was respectively reacted with isonitriles **1a-d** and ammonium formate in MeOH to afford N^{α} -formyl Adm-containing C-alkylamides and dipeptides **2a-d**. Formamides **2a-d** were converted into the corresponding isonitriles **3a-d** in excellent yields using $POCl_3$ and TEA, and elongated by the Ugi procedure to the corresponding N^{α} -formyl Adm di- and tripeptides **4a-d**.

3.2 | Crystal-state conformational analysis

The 3D-structures of the Adm-containing di- and tripeptides **2d** and **4a-d** were solved by X-ray diffraction (Figures 1–5). The C-terminal substituent effects on peptide conformation with specific attention to γ -turn formation were assessed by evaluation of ϕ and ψ backbone torsion angles (Table 1) and intramolecular hydrogen-bond distances between amide (peptide) carbonyl and N-H groups (Table 2). Composed of achiral Adm, Gly and Aib residues, the five peptides were expected to crystallize in two enantiomeric conformers. For example, peptides **2d**, **4a** and **4b** crystallized in centrosymmetric space groups. On the other hand, peptides **4c** and **4d** crystallized in one of the

SCHEME 1 Solution-phase syntheses of N^α-formyl Adm-containing di- and tripeptides



Sohncke space groups in which molecules of only one handedness occur,^[44] due to the rather uncommon phenomenon termed *spontaneous resolution*.^[45] Crystals of peptides **4c** and **4d** were affected by twinning through inversion.

In the five structures, the amide, peptide, and ester bonds, all adopt the usual *trans* isomer ($\omega = 180^\circ$) without significant deviation ($|\Delta\omega| \leq 7.9^\circ$) from the ideal planarity.

In the molecule arbitrarily selected as the asymmetric unit in the centrosymmetric structure of the dipeptide HCO-Adm-Aib-OMe composed of two achiral, C^α-tetrasubstituted α -amino acids (**2d**; Figure 1), the Adm residue adopts a left-handed, highly distorted helical conformation [$\phi_1, \psi_1 = 72.41(16)^\circ, 75.06(13)^\circ$] (Table 1). The C-terminal Aib

residue is also helical, but of opposite screw sense with respect to the preceding residue [$\phi_2, \psi_2 = -48.05(16)^\circ, -47.20(15)^\circ$]. The overall backbone of **2d** can be described as S-shaped.^[46,47] Without intramolecular hydrogen bonds, the amide N-H of the Adm and Aib residues form respectively intermolecular hydrogen bonds with the carbonyl oxygens of the Adm and formyl groups in a $(-x + 1/2, y + 1/2, -z + 1/2)$ symmetry-related molecule (Table 2), the packing mode

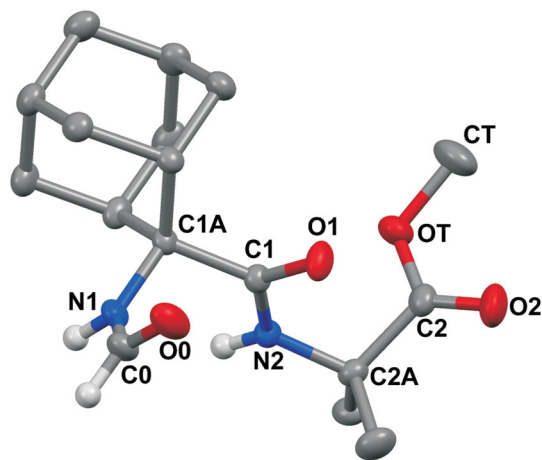


FIGURE 1 X-Ray diffraction structure of HCO-Adm-Aib-OMe (**2d**). Displacement ellipsoids are drawn at the 30% probability level. Most hydrogen atoms are omitted for clarity

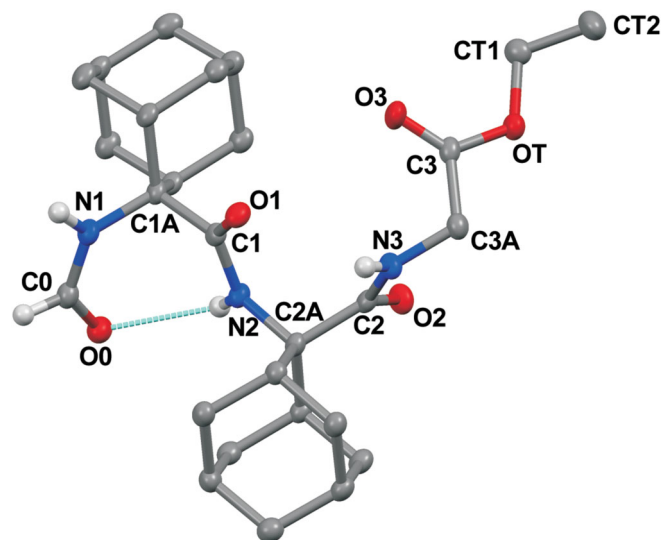


FIGURE 2 X-Ray diffraction structure of HCO-(Adm)₂-Gly-OEt (**4a**). Displacement ellipsoids are drawn at the 30% probability level. Most hydrogen atoms are omitted for clarity. The single C=O \cdots H-N intramolecular hydrogen bond is indicated by a dashed line

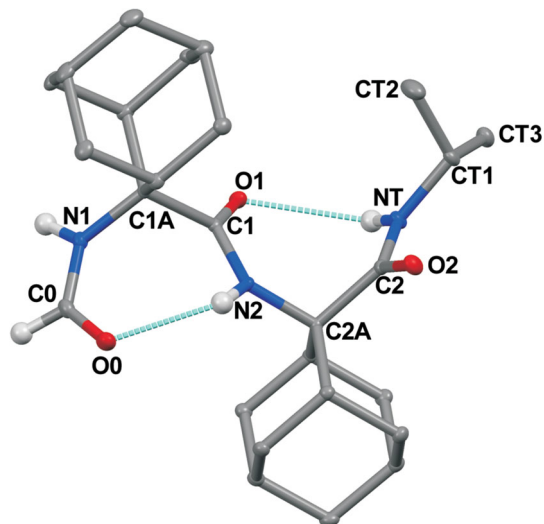


FIGURE 3 X-Ray diffraction structure of HCO-(Adm)₂-NHiPr (4b). Displacement ellipsoids are drawn at the 30% probability level. Most hydrogen atoms are omitted for clarity. The two C=O \cdots H–N intramolecular hydrogen bonds are indicated by dashed lines

featuring rows of molecules, related through a 2-fold axis, along the *b* direction. Packing is favored by van der Waals interactions.

The X-ray diffraction structure of the less bulky of the two tripeptides studied, HCO-(Adm)₂-Gly-OEt (4a, Figure 2), is stabilized by a single *i* + 2 to *i* intramolecular hydrogen bond between the formyl carbonyl oxygen and the Adm(2) amide N-H (Table 2) in a 7-membered γ -turn conformation possessing characteristic backbone ϕ_1 , ψ_1 torsion angles [–75.9(3)°, 79.2(3)°] for the N-terminal Adm(1) residue (Table 1).^[23,24,29] Moreover, the values for the Adm(2) backbone torsion angles are rather close to those expected for a

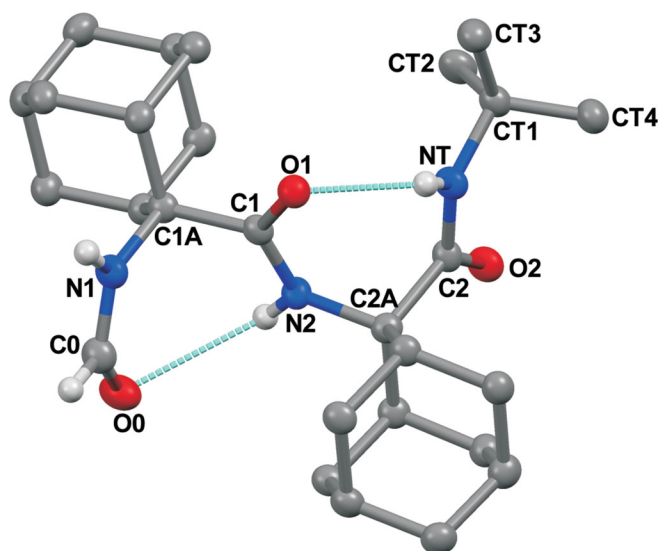


FIGURE 4 X-Ray diffraction structure of HCO-(Adm)₂-NHtBu (4c). Displacement ellipsoids are drawn at the 30% probability level. Most hydrogen atoms are omitted for clarity. The two C=O \cdots H–N intramolecular hydrogen bonds are indicated by dashed lines

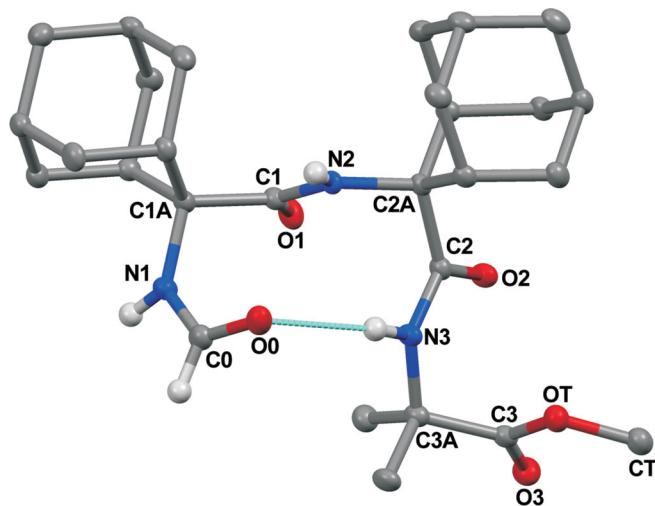


FIGURE 5 X-Ray diffraction structure of HCO-(Adm)₂-Aib-OMe (4d). Displacement ellipsoids are drawn at the 30% probability level. Most hydrogen atoms are omitted for clarity. The single C=O \cdots H–N intramolecular hydrogen bond is indicated by a dashed line

regular γ -turn. Specifically, the ϕ_2 value [–69.2(3)°] is appropriate for a γ -turn conformation, but the ψ_2 value [96.8(3)°] is slightly too large, suggesting formation of an “open” γ -turn. In corroboration, the intramolecular H \cdots O distance (2.60 Å) between the N-terminal Adm(1) carbonyl oxygen and the Gly(3) N-H exceeds slightly the commonly accepted limit for the onset of a hydrogen bond (≤ 2.50 Å).^[48–50] The C-terminal Gly(3) residue is *semi*-extended [ϕ_3 , $\psi_3 = 84.5(3)^\circ$, –158.4(2)°]. Two intermolecular hydrogen bonds between the N-terminal Adm(1) amide N-H and the Adm(2) carbonyl of a translationally equivalent molecule (*x*-1, *y*, *z*) generate molecular rows along the *a* direction. Another intermolecular hydrogen bond is observed between opposing Gly(3) amide N-H and Gly(3) ester C=O groups, forming a (1-*x*, 1-*y*, 1-*z*) centrosymmetric pair (Table 2).

Peptides exhibiting two consecutive γ -turns are characteristic of incipient γ -helices and relatively rare.^[29] The crystal-state conformers of dipeptide alkyl amides HCO-(Adm)₂-NHR 4b and 4c (R = *i*Pr and *t*Bu, Figures 3 and 4) illustrate the potential for the Adm residue to favor such geometry. Both 4b and 4c feature a classical 7-membered ring γ -turn structure with an *i* + 2 to *i* intramolecular hydrogen bond between the formyl C=O and the Adm(2) peptide N-H groups (Table 2). In both 4b and 4c, the N-terminal Adm(1) residue adopts characteristic ϕ_1 and ψ_1 torsion angles [76.49(12)°, –79.37(10)° for 4b, and –77.5(5)°, 84.8(4)° for 4c (Table 1)]. Moreover, the C-terminal Adm(2) residue adopts γ -turn geometry in both dipeptides, which exhibit *i* + 2 to *i* intramolecular hydrogen-bond distances between the N-terminal Adm(1) carbonyl oxygen and the alkyl amide N-H (2.40 Å and 2.10 Å, respectively, for 4b and 4c, Table 2). Although the ϕ_2 torsion angle matches ideal γ -turn geometry in both dipeptides, and the ψ_2 torsion angle is regular for 4c [70.5(4)°], ψ_2 deviates significantly [–88.12(10)°] from the ideal in 4b (Table 1). In both structures, an intermolecular hydrogen bond is observed between the Adm(1) amide N-H and Adm(2) C=O groups in symmetry-related molecules

TABLE 1 Backbone ϕ and ψ torsion angles ($^{\circ}$) observed for the X-ray diffraction structures of N $^{\alpha}$ -formyl Adm-containing di- and tripeptides

Entry	Peptide sequence	ϕ_1	ψ_1	ϕ_2	ψ_2	ϕ_3	ψ_3	Type of turn
2d	HCO-Adm-Aib-OMe	72.41 (16)	75.06 (13)	-48.05 (16)	-47.20 (15)			—
4a	HCO-(Adm) $_2$ -Gly-OEt	-75.9 (3)	79.2 (3)	-69.2 (3)	96.8 (3)	84.5 (3)	-158.4 (2)	One γ -turn, one "open" γ -turn
4b	HCO-(Adm) $_2$ -NH i Pr	76.49 (12)	-79.37 (10)	69.79 (11)	-88.12 (10)			Two consecutive γ -turns
4c	HCO-(Adm) $_2$ -NH t Bu	-77.5 (5)	84.8 (4)	-74.3 (4)	70.5 (4)			Two consecutive γ -turns
4d	HCO-(Adm) $_2$ -Aib-OMe	63.1 (5)	-96.9 (4)	-51.4 (5)	-49.6 (5)	56.2 (5)	43.9 (5)	Distorted type-II' β -turn

Abbreviations: Aib, α -aminoisobutyric acid; OMe, methoxy; OEt, ethoxy; NH i Pr, *iso*-propylamino; NH t Bu, *tert*-butylamino.

(Table 2), which pack respectively along the a direction and around the 3_1 screw axis in the crystals of **4b** and **4c**.

In the crystal structure of the bulkier tripeptide HCO-(Adm) $_2$ -Aib-OMe **4d** (Figure 5), the -Adm-Adm- dipeptide adopts ϕ and ψ torsion angles [63.1(5) $^{\circ}$, -96.9(4) $^{\circ}$; -51.4(5) $^{\circ}$, -49.6(5) $^{\circ}$] (Table 1) which are reminiscent of the $i + 1$ and $i + 2$ residues of an ideal 10-membered ring type-II' β -turn structure (60 $^{\circ}$, -120 $^{\circ}$; -90 $^{\circ}$, 0 $^{\circ}$).^[7-12] In spite of significant distortion, an $i + 3$ to i intramolecular hydrogen bond (2.20 Å) is observed between the formyl C=O and Aib(3) peptide N-H groups (Table 2). The conformation adopted by the C-terminal Aib(3) residue is helical [ϕ_3 , ψ_3 = 56.2(5) $^{\circ}$, 43.9(5) $^{\circ}$] with a screw-sense reversal with respect to the preceding Adm(2) residue. As a result, the C-terminal -Adm(2)-Aib(3)- sequence adopts an S-shaped folding^[46,47] similar to that observed for dipeptide **2d**. However, in the case of **4d** the torsion angles of the two residues are closer to the values typical, respectively, for a right-handed and a left-handed regular α -helical conformation than those of **2d**. Tripeptide **4d** packs with an intermolecular hydrogen bond between the N-terminal Adm(1) N-H and the central Adm(2) C=O oxygen group of a (- x , $\frac{1}{2} + y$, $\frac{1}{2} - z$) symmetry-related molecule (Table 2).

Previously, conformational energy calculations using density functional theory [performed using the B3LYP functional combined with the 6-31 + G(d,p) basis set] had predicted that after the most stable

consecutive γ -turn conformer, Ac-(Adm) $_2$ -NHMe could adopt a distorted type-II (II') β -turn with backbone torsion angles differing less than 10 $^{\circ}$ from those found for tripeptide **4d**.^[30] This nonhelical type of turn had however not been previously reported experimentally for N-acyl Adm dipeptide amide sequences. Overall, the crystal structures of **4b-d** confirm that the double γ -turn and type-II (II') β -turn conformations are energetically accessible for -Adm-Adm- dipeptide sequences. Although the ϕ and ψ torsion angles of the N-terminal Adm(1) residue in **4d** are rather close to those of a regular γ -turn, the distance (2.67 Å) between the formyl C=O oxygen and the Adm(2) peptide N-H is too long for an intramolecular hydrogen bond.

An overlay of the four structures containing the -(Adm) $_2$ - sequence, namely HCO-(Adm) $_2$ -Gly-OEt (**4a**), HCO-(Adm) $_2$ -NH i Pr (**4b**), HCO-(Adm) $_2$ -NH t Bu (**4c**), and HCO-(Adm) $_2$ -Aib-OMe (**4d**) is illustrated in Figure 6. For **4b** and **4d**, the (- x , - y , - z) counterparts are shown for the molecules to which torsion angles reported in Table 1 refer. In all four structures, the ϕ torsion angle of the N-terminal Adm residue is negative and ψ is positive, to enable a clear visual comparison. The maximum overlap of the N-terminal Adm residue (positioned at the top) was used to superimpose the four structures. Three of them, **4a**, **4b**, and **4c**, show close proximity also for their N-terminal formyl group and the second Adm residue. The outlier is **4d**, owing to its (distorted) β -turn fold,

TABLE 2 Intramolecular and intermolecular hydrogen-bond parameters for the X-ray diffraction structures of N $^{\alpha}$ -formyl Adm-containing di- and tripeptides

Entry	Peptide sequence	Type	Donor D-H	Acceptor A	Distance (Å) D...A	Distance (Å) H...A	Angle ($^{\circ}$) D-H...A	Symmetry equivalence of A
2d	HCO-Adm-Aib-OMe	Intermolecular	N1-H1	O1	2.8448 (14)	2.02	159.9	- $x + 1/2$, $y + 1/2$, - $z + 1/2$
		Intermolecular	N2-H2	O0	3.0822 (16)	2.23	168.4	- $x + 1/2$, $y + 1/2$, - $z + 1/2z$
4a	HCO-(Adm) $_2$ -Gly-OEt	Intramolecular	N2-H2	O0	2.935 (3)	2.31	128.1	x , y , z
		Intermolecular	N1-H1	O2	2.851 (3)	1.98	172.9	$x - 1$, y , z
		Intermolecular	N3-H3	O3	3.163 (3)	2.39	147.1	$1 - x$, $1 - y$, $1 - z$
4b	HCO-(Adm) $_2$ -NH i Pr	Intramolecular	N2-H2	O0	2.9167 (11)	2.22	137.4	x , y , z
		Intramolecular	NT-HT	O1	2.9214 (11)	2.40	120.0	x , y , z
		Intermolecular	N1-H1	O2	2.9026 (12)	2.03	163.0	$x - 1$, y , z
4c	HCO-(Adm) $_2$ -NH t Bu	Intramolecular	N2-H2	O0	3.118 (5)	2.56	122.3	x , y , z
		Intramolecular	NT-HT	O1	2.756 (5)	2.10	131.0	x , y , z
		Intermolecular	N1-H1	O2	2.833 (5)	2.02	153.0	$y - x$, $1 - x$, -1/3 + z
4d	HCO-(Adm) $_2$ -Aib-OMe	Intramolecular	N3-H3	O0	3.038 (5)	2.20	163	x , y , z
		Intermolecular	N1-H1	O2	2.859 (5)	2.05	156	- x , $1/2 + y$, $1/2 - z$

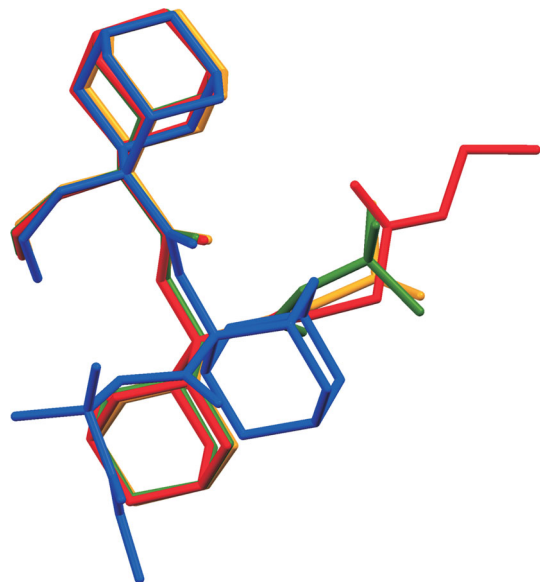


FIGURE 6 Overlay of the X-ray diffraction structures of HCO-(Adm)₂-Gly-OEt (**4a**) (red), HCO-(Adm)₂-NH*i*Pr (**4b**) (orange), HCO-(Adm)₂-NH*t*Bu (**4c**) (green), and HCO-(Adm)₂-Aib-OMe (**4d**) (blue). See text for details

characterized *inter alia* by the helical backbone torsion angles adopted by Adm(2).

4 | DISCUSSION

The backbone conformations of four N^α-formyl Adm homo-dipeptide sequences possessing various C-terminal secondary amide components were determined in the crystal state using X-ray diffraction. Moreover, the corresponding -Adm-Aib- hetero-dipeptide sequence with a C-terminal ester group was also investigated. Although the results of the present study are limited to similar sequences that may largely depend on the crystallization solvent and crystal packing forces, certain trends do emerge from examination of the influences exerted by the nature of the C-terminal groups.

Two ϕ and ψ regions of the Ramachandran map were predominantly found to be explored by the Adm residues. In the most extensively populated region, the two backbone torsion angles ($\pm 60^\circ < \phi < \pm 80^\circ$ and $\pm 70^\circ < \psi < \pm 95^\circ$) are characterized by *opposite* sign. Within this region, ϕ and ψ values of comparable magnitude (up to $\pm 80^\circ$) are typical of the central residue of an intramolecularly hydrogen-bonded γ -turn and are also observed in consecutive γ -turns of incipient γ -helices, whereas ψ values larger than $\pm 80^\circ$ are associated with slightly distorted (open) γ -turns and may be as well tolerated at position $i + 1$ of a type-II (II') β -turn. The second region, characterized by ϕ and ψ torsion angles with the *same* sign and $\psi > \pm 50^\circ$, may host the $i + 2$ position of a distorted type-II (II') β -turn. The steric bulk of the Adm residue apparently restricts the ϕ and ψ values from adopting conformations common to homo-peptides based on C^{α,α}-disubstituted glycines with smaller substituents, including the 3₁₀-helix, both corner

positions of type-III (III')/I (I') β -turns, and all types of extended structures, including the *semi*-extended, type-II poly-(Pro)_n helix and the fully extended structure.^[16–18]

The observed backbone topologies concur with those previously reported in X-ray diffraction analyses of Adm peptides, including Adm homo-tripeptides,^[30,31] in which incipient γ -helices as well as a rare isolated α -turn with average ϕ and ψ torsion angle values of the *same* sign [57.1° , 51.7°] were observed.^[51–55] The two achiral amino acid components in the -CO-Adm-Aib-OR sequences analyzed in the present study, peptides **2d** and **4d**, both exhibit S-shaped helical conformations with *opposite* screw senses. The bias for this conformation may in part be due to the extremely strong propensity for the Aib residue to adopt helical geometry.^[1–6] Whether this 3D-structural disposition is restricted to isolated N^α-acyl dipeptide esters or may propagate to longer sequences (e.g., -[Adm-Aib]_n-, $n > 1$) remains to be investigated.

The steric bulk of the C-terminal amino substituent (-NHR) appears to play a role on the conformation of the -Adm-Adm- dipeptide sequence. In contrast to the influences of Aib residues observed in dipeptide **2d** and tripeptide **4d** discussed above, those of an additional Adm residue (in homo-tripeptides)^[31] and *t*Bu in dipeptide **4c** tend to favor a regular γ -turn conformation. On the other hand, less bulky di- and trisubstituted carbons [e.g., in Cbz-Adm-Gly-OEt,^[30] and Gly in tripeptide **4a**; *i*Pr in dipeptide **4b**, in HCO-(Adm)₃-NH-Pr,^[31] and in "N₃"-(Adm)₃-NH-Pr^[30]; and Ala in Cbz-Adm-L-Ala-OMe,^[28]] distort the ideal γ -turn torsion angle values by rotating the Adm C-terminal amide away from serving as a correctly positioned N-H hydrogen-bond donor. This 3D-structural change may generate an open γ -turn and even an α -helical conformation. In addition to steric bulk, the dipole interaction of ester moieties may likely dictate rotation about the Adm C-terminal amide to influence potential for adopting ideal γ -turn backbone torsion angles. In this context, this study offers light on design elements for favoring specific peptide secondary structures using Adm as a novel C^{α,α}-dialkylglycine residue.

ACKNOWLEDGMENTS

This research was supported by the Natural Sciences and Engineering Research Council of Canada (NSERC) Discovery Grant RGPIN-06647, the FRQNT Centre in Green Chemistry and Catalysis (CGCC) Strategic Cluster RS-171310, and the Université de Montréal. We thank Mr. T. Maris (X-ray diffraction), C. Malveau, Dr. P. Aguiar and S. Bilodeau (NMR spectroscopy), Dr. A. Fürtös, K. Gilbert, and M.-C. Tang (mass spectrometry) from Université de Montréal Laboratories for their assistance in analyses.

ORCID

Fatemeh M. Mir  <https://orcid.org/0000-0002-0653-9010>

Marco Crisma  <https://orcid.org/0000-0003-3552-4106>

Claudio Toniolo  <https://orcid.org/0000-0002-2327-1423>

William D. Lubell  <https://orcid.org/0000-0002-3080-2712>

REFERENCES

- [1] N. Shamala, R. Nagaraj, P. Balaran, *Chem. Commun.* **1978**, 996.
- [2] E. Benedetti, A. Bavoso, B. Di Blasio, V. Pavone, C. Pedone, M. Crisma, G. M. Bonora, C. Toniolo, *J. Am. Chem. Soc.* **1982**, *104*, 2437.
- [3] C. Toniolo, E. Benedetti, *Macromolecules* **1991**, *24*, 4004.
- [4] I. L. Karle, *Biopolymers* **2001**, *60*, 351.
- [5] R. Gessmann, H. Brückner, K. Petratos, *J. Pept. Sci.* **2016**, *22*, 76.
- [6] J. Solá, M. Helliwell, J. Clayden, *Biopolymers* **2011**, *95*, 62.
- [7] C. M. Venkatachalam, *Biopolymers* **1968**, *6*, 1425.
- [8] J. A. Geddes, K. B. Parker, E. D. T. Atkins, E. Beighton, *J. Mol. Biol.* **1968**, *32*, 343.
- [9] P. N. Lewis, F. A. Momany, H. A. Scheraga, *Biochim. Biophys. Acta* **1973**, *303*, 211.
- [10] C. Toniolo, *CRC Crit. Rev. Biochem.* **1980**, *9*, 1.
- [11] J. A. Smith, L. G. Pease, *CRC Crit. Rev. Biochem.* **1980**, *8*, 315.
- [12] G. D. Rose, L. M. Gierasch, J. A. Smith, *Adv. Protein Chem.* **1985**, *37*, 1.
- [13] L. Pauling, R. B. Corey, H. R. Branson, *Proc. Natl. Acad. Sci. USA* **1951**, *37*, 205.
- [14] C. Toniolo, E. Benedetti, *Trends Biochem. Sci.* **1991**, *16*, 350.
- [15] C. Toniolo, M. Crisma, F. Formaggio, C. Peggion, *Biopolymers* **2001**, *60*, 396.
- [16] E. Benedetti, V. Barone, A. Bavoso, B. Di Blasio, F. Lelj, V. Pavone, C. Pedone, G. M. Bonora, C. Toniolo, M. Leplawy, *Biopolymers* **1988**, *27*, 357.
- [17] M. Tanaka, *Chem. Pharm. Bull. (Tokyo)* **2007**, *55*, 349.
- [18] C. Peggion, A. Moretto, F. Formaggio, M. Crisma, C. Toniolo, *Biopolymers* **2013**, *100*, 621.
- [19] A. P. Marchand, *Science* **2003**, *299*, 52.
- [20] H. Schwertfeger, A. A. Fokin, P. R. Schreiner, *Angew. Chem. Int. Ed.* **2008**, *47*, 1022.
- [21] L. Wanka, K. Iqbal, P. R. Schreiner, *Chem. Rev.* **2013**, *113*, 3516.
- [22] M. A. Gunawan, J.-C. Hierso, D. Poinot, A. A. Fokin, N. A. Fokina, B. A. Tkachenko, P. R. Schreiner, *New J. Chem.* **2014**, *38*, 28.
- [23] G. Némethy, M. P. Printz, *Macromolecules* **1972**, *5*, 755.
- [24] B. W. Matthews, *Macromolecules* **1972**, *5*, 818.
- [25] J. L. Flippen-Anderson, I. L. Karle, *Biopolymers* **1976**, *15*, 1081.
- [26] E. J. Milner-White, B. M. Ross, R. Ismail, K. Belhadj-Mostefa, R. Poet, *J. Mol. Biol.* **1988**, *204*, 777.
- [27] A. I. Jiménez, G. Ballano, C. Cativiela, *Angew. Chem. Int. Ed.* **2005**, *44*, 396.
- [28] R. Kishore, P. Balaran, *Biopolymers* **1985**, *24*, 2041.
- [29] M. Crisma, M. De Zotti, A. Moretto, C. Peggion, B. Drouillard, K. Wright, F. Couty, C. Toniolo, F. Formaggio, *New J. Chem.* **2015**, *39*, 3208.
- [30] D. Mazzier, L. Grassi, A. Moretto, C. Alemán, F. Formaggio, C. Toniolo, M. Crisma, *J. Pept. Sci.* **2017**, *23*, 346.
- [31] F. M. Mir, M. Crisma, C. Toniolo, W. D. Lubell, unpublished.
- [32] Y. Kuroda, H. Ueda, H. Nozawa, H. Ogoshi, *Tetrahedron Lett.* **1997**, *38*, 7901.
- [33] J. Donohue, *Proc. Natl. Acad. Sci. USA* **1953**, *39*, 470.
- [34] T. Yamada, Y. Omote, Y. Yamanaka, T. Miyadawa, S. Kuwata, *Synthesis* **1998**, *1998*, 991.
- [35] T. Pirali, G. C. Tron, G. Masson, J. Zhu, *Org. Lett.* **2007**, *9*, 5275.
- [36] S. Kotha, M. Behera, P. Khedkar, *Tetrahedron Lett.* **2004**, *45*, 7589.
- [37] M. C. Burla, R. Caliendo, B. Carrozzini, G. L. Cascarano, C. Cuocci, C. Giacobazzo, M. Mallamo, A. Mazzone, G. Polidori, *J. Appl. Crystallogr.* **2015**, *48*, 306.
- [38] G. M. Sheldrick, *Acta Crystallogr. A* **2015**, *71*, 3.
- [39] G. M. Sheldrick, *Acta Crystallogr. C* **2015**, *71*, 3.
- [40] L. J. Bourhis, O. V. Dolomanov, R. J. Gildea, J. A. K. Howard, H. Puschmann, *Acta Crystallogr. A* **2015**, *71*, 59.
- [41] F. Formaggio, Q. B. Broxterman, C. Toniolo, in *Houben-Weyl, Methods of Organic Chemistry*, Vol. E22c, *Synthesis of Peptides and Peptidomimetics* (Eds: M. Goodman, A. Felix, L. Moroder, C. Toniolo), Thieme, Stuttgart, Germany **2003**, p. 292.
- [42] H. Brückner, M. Curre, in *Second Forum on Peptides*, Vol. 174 (Eds: A. Aubry, M. Marraud, B. Vitoux), Libbey Eurotext, Paris **1989**, p. 251.
- [43] S. Samsoniya, D. Zurabishvili, T. Bukia, G. Buzaladze, M. Lomidze, E. Elizbarashvili, U. Kazmaier, *Bull. Georgian Natl. Acad. Sci.* **2014**, *8*, 85.
- [44] M. Nespolo, M. I. Aroyo, B. Souvignier, *J. Appl. Crystallogr.* **2018**, *51*, 1481.
- [45] L. Pérez-García, D. B. Amabilino, *Chem. Soc. Rev.* **2002**, *31*, 342.
- [46] V. K. Goel, M. Guha, A. P. Baxia, S. Dey, T. P. Singh, *J. Mol. Struct.* **2003**, *658*, 135.
- [47] E. Vijayaraghavan, V. K. Goel, S. Dey, T. P. Singh, *Struct. Chem.* **2005**, *16*, 445.
- [48] R. Taylor, O. Kennard, W. Versichel, *Acta Crystallogr. B* **1984**, *40*, 280.
- [49] C.-H. Görbitz, *Acta Crystallogr. B* **1989**, *45*, 390.
- [50] I. Y. Torshin, I. T. Weber, R. W. Harrosin, *Protein Eng.* **2002**, *15*, 359.
- [51] V. Pavone, G. Gaeta, A. Lombardi, F. Nastro, O. Maglio, C. Isernia, M. Saviano, *Biopolymers* **1996**, *38*, 705.
- [52] K.-C. Chou, *Biopolymers* **1997**, *42*, 837.
- [53] C. Ramakrishnan, D. V. Nataraj, *J. Pept. Sci.* **1998**, *4*, 239.
- [54] M. Narita, K. Sode, S. Ohuchi, *Bull. Chem. Soc. Jpn* **1999**, *72*, 1807.
- [55] B. Dasgupta, L. Pal, G. Basu, P. Chakrabarti, *Proteins: Struct. Funct. Bioinform.* **2004**, *55*, 305.

SUPPORTING INFORMATION

Additional supporting information may be found online in the Supporting Information section at the end of this article.

How to cite this article: Mir FM, Crisma M, Toniolo C, Lubell WD. Influence of the C-terminal substituent on the crystal-state conformation of Adm peptides. *Pept Sci.* 2019; e24121. <https://doi.org/10.1002/pep2.24121>